Method to measure the viscosity of nanometer liquid films from the surface fluctuations

Zhaohui Yang,[1] Chi-Hang Lam,[2] Elaine DiMasi,[3] Nathalie Bouet,[1] Jean Jordan-Sweet,[4] and Ophelia K. C. Tsui[1,a)]
[1]*Department of Physics, Boston University, Boston, Massachusetts 02215, USA*
[2]*Department of Applied Physics, Hong Kong Polytechnic University, Hung Hom, Hong Kong*
[3]*National Synchrotron Light Source, Brookhaven National Laboratory, Upton, New York 11973, USA*
[4]*IBM Research Division, Thomas J. Watson Research Center, Yorktown Heights, New York 10598, USA*

(Received 13 March 2009; accepted 3 June 2009; published online 23 June 2009)

We describe a method to measure the viscosity of polystyrene liquid films with thicknesses ~5 and ~80 nm spin-cast on oxide-coated silicon. In this method, temporal evolution of the film surface is monitored and modeled according to the dynamics of the surface capillary waves. Viscosities obtained from the ~80 nm films display an excellent agreement with those of the bulk polymer, but those from the ~5 nm films are up to 10^6 times reduced. By modeling the data to the Vogel–Fulcher–Tammann relation, we find that the observations are consistent with the thickness dependence of the glass transition temperature previously reported of these films. © *2009 American Institute of Physics*. [DOI: 10.1063/1.3158956]

A broad range of liquids undergo the glass transition upon cooling.[1] In the glass transition, the viscosity of a liquid increases rapidly to $\sim 10^{12}$ Pa s past the glass transition temperature, T_g. Beyond that, any fluid flow inside the liquid occurs so slowly that the liquid is practically rigid as a solid and termed a glass.[1] Under nanoconfinement, studies have shown that the T_g of a glass-forming material can be quite different from the bulk as the size of confinement is decreased below ~20 nm.[2,3] But so far, the mechanism underpinning the phenomenon is unsettled. Although important clues are expected from the size dependence of the manner by which the viscosity increases upon cooling toward the T_g,[3] viscosity measurements of nanoconfined liquids are scarce. For nanoconfined liquid films, there have been several viscosity measurements, primarily by x-ray photon correlation spectroscopy (XPCS)[3–5] and dewetting.[3,6] But there are limitations. In XPCS, the detector response and temporal instability of the synchrotron beam[5] restrict the measurement time to a dynamic range of three decades.[4,5] In dewetting measurements, limitation arises from the increased number density of holes nucleated in the film with decreasing thickness, h. If dense enough, the holes can prevent the holes opening process to be followed for an adequate period of time.[3] The smallest film thickness studied by these methods was 27 nm,[6] where the confinement effect is still insignificant.

In this letter, we describe a method by which we can measure the viscosity of liquid films down to $h \approx 5$ nm. Low molecular-weight (M_w) polystyrene (PS) spun-cast on oxide-coated silicon is chosen for illustration. Previous studies[7,8] showed that these films are unstable and roughen spontaneously upon heating. We deduce the viscosity of the films by measuring the temporal evolution of the film surface and then modeling the data by assuming the dynamics to be due to the surface capillary waves subject to spinodal instability[9] and thermal noise.[7] In brief, in the lubrication approximation, pertinent to typical experiments, the linear stability analysis, corresponding to the presumption, $h(\boldsymbol{r},t) \approx h + \Sigma \boldsymbol{q}_\parallel \delta h(\boldsymbol{q}_\parallel,t)\exp(i\boldsymbol{q}_\parallel \cdot \boldsymbol{r})$, with

$$\delta h(\boldsymbol{q}_\parallel,t) = \delta h(\boldsymbol{q}_\parallel)\exp[\Gamma(q_\parallel)t], \tag{1}$$

(where $\delta h(\boldsymbol{q}_\parallel,t) \ll h$; $\boldsymbol{r}=(x,y)$ and $\boldsymbol{q}_\parallel=(q_x,q_y)$ are, respectively, the in-plane position and wave vector) leads to the following dispersion relation:[9]

$$\Gamma(q_\parallel) = \frac{-h^3}{3\eta}[\gamma q_\parallel^4 + G''(h)q_\parallel^2]. \tag{2}$$

In Eq. (2), η is the viscosity, γ is the surface tension, and $G(h)$ is the interfacial potential of the film.[8] For the films with $G''(h)<0$, $\Gamma(q_\parallel)>0$ for the modes with $q_\parallel < (-G''/\gamma)^{1/2}$.[10] Given Eq. (1), $\Gamma(q_\parallel)>0$ means that $|\delta h(\boldsymbol{q}_\parallel,t)|^2$ grows exponentially with time. This, constituting the spinodal process,[7,9] causes the films to be unstable against spontaneous roughening. To incorporate the effects of thermal noise, we consider the evolution of the capillary modes to be a thermalization process instead of simple spinodal following:

$$|\delta h(\boldsymbol{q}_\parallel,t)|^2 = |\delta h(\boldsymbol{q}_\parallel,0)|^2 + (|\delta h(\boldsymbol{q}_\parallel,\infty)|^2 - |\delta h(\boldsymbol{q}_\parallel,0)|^2)(1-e^{2\Gamma(q_\parallel)t}), \tag{3}$$

where $|\delta h(q_\parallel,\infty)|^2 \equiv k_B T/[\gamma q^2 + G''(h)]$. The physical origin of Eq. (3) can be appreciated by comparing it with the analogous expression describing the time variation of the charge stored in a capacitor being charged at a time constant of $1/\Gamma(q_\parallel)$. For the interfacial potential, $G(h)$, we use the van der Waals potential previously reported for the PS-SiO_x-Si films.[8] From Refs. 7 and 8, $G''(h)<0$ when $h<\sim 250$ nm. In this experiment, we study films with thickness between 4 and 80 nm so Eqs. (2) and (3) are applicable. We model the surface evolution data by these equations with γ fixed at 30 mN/m and only the viscosity η varied as the fitting parameter.

PS homopolymer with $M_w = 2.4$ kg/mol below the entanglement limit and polydispersity = 1.06 was used. Solu-

a)Author to whom correspondence should be addressed. Electronic mail: okctsui@bu.edu.

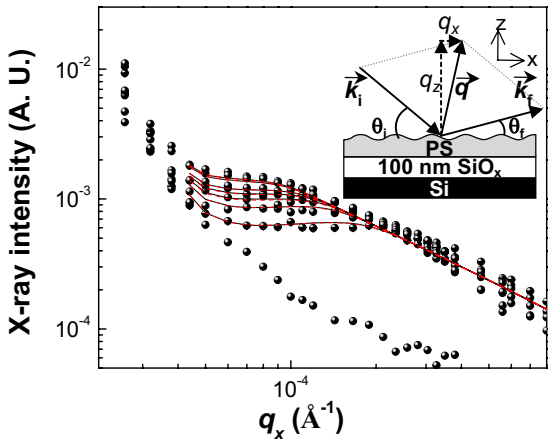

FIG. 1. (Color online) (Main panel) Time-resolved GISAXS spectra (filled circles) obtained from an 80 nm film annealed at 368 K, with q_z kept at 0.12 Å^{-1}. The annealing times are (from the bottom) 0, 414, 1246, 2096, 2945, 3810, 6720, and 7630 s. The solid lines are the model lines from least-square fitting. The dashed lines, essentially overlapping with the solid lines, are analogous model lines but with $G''(h)$ set to zero. (Inset) Schematic reciprocal space diagram of the GISAXS experiment. The incident and scattered wave vectors are $\boldsymbol{k}_i$ and $\boldsymbol{k}_f$, with incident and exit angle, θ_i and θ_f, respectively.

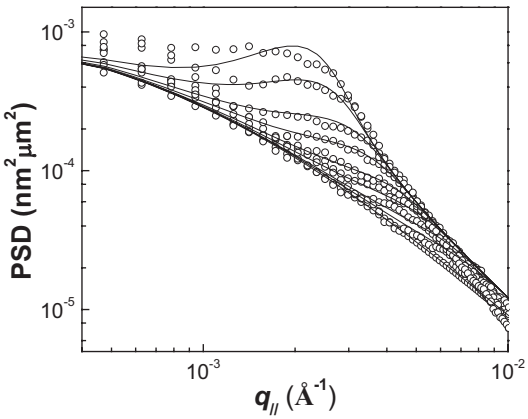

FIG. 2. Time-resolved AFM surface spectra of a 4 nm film annealed at 334 K. The annealing times are (from the bottom) 0, 10, 20, 60, 120, 240, 480, 1080, and 1920 s. The solid lines are the best fitted model lines.

tions of this polymer in toluene were spun-cast onto silicon covered with a 100-nm-thick SiO_x to produce PS films with thicknesses equal 4 to 80 nm. The silicon wafers were previously cleaned by immersing them in a solution mixture of H_2SO_4 and H_2O_2 (7:3 by volume) at 403 K for 10 min, followed by exposure to an oxygen plasma for 20 min. The samples were heated on a temperature-controlled hot stage enclosed inside a sealed chamber filled with helium or nitrogen at a slight positive pressure. Grazing incidence small-angle x-ray scattering (GISAXS) was performed at beamline X6B of the National Synchrotron Light Source (NSLS) at the Brookhaven National Laboratory. The scattering geometry is shown in the inset of Fig. 1 in which $\boldsymbol{q}=\boldsymbol{k}_f-\boldsymbol{k}_i=(q_x,0,q_z)$ is the scattering wave vector. The wavelength of the x-ray was 1.54 Å. To acquire the surface spectrum for the sample, the intensity of the scattered x-ray was recorded with a scintillation detector as q_x was scanned while q_z was kept at 0.12 Å^{-1}. Two pairs of slits, constraining the synchrotron beam along z and y, were placed just before the sample. The slits along z were tightly closed, enabling resolutions of 0.0016 and 0.000 024 Å^{-1} in q_z and q_x, respectively. The slits along y, on the other hand, were widely open to allow the maximum signal to the detector. The GISAXS measurements were performed *in situ* as the sample was heated in real-time. The average scan time for each spectrum was 12 min. We adopted the central time of each scan as the annealing time. With the setup we have for GISAXS, the signal becomes too small to measure for $q_x > \sim 10^{-3}$ Å^{-1}. But for the $h \approx 5$ nm films, the relevant features extend to $q_{\parallel} \sim 10^{-2}$ Å^{-1}. So tapping mode atomic force microscopy (AFM) was used. We carried out the measurements *ex situ* with the samples quenched at various cumulative annealing times. The topographic images obtained were converted to the corresponding surface spectrum (or power spectral density) by first multiplying them with a Welch function then Fourier transforming and radial averaging the result as detailed before.[7]

Shown in the main panel of Fig. 1 (solid circles) are the time-resolved GISAXS surface spectra obtained from an $h=80$ nm film annealed at 368 K. Analogous spectra obtained by AFM from an $h=4$ nm film at 334 K are shown in Fig. 2 (open circles). The solid lines represent the least-square fit to the data by Eq. (3). For the GISAXS data in Fig. 1, Eq. (3) is additionally integrated along y to take into account the fact that the slits are widely open in the y direction. In the $q_{\parallel} < \sim 4 \times 10^{-4}$ Å^{-1} range, however, the data is usually dominated by the finite coherence length of the x-ray beam[11] and ignored in the analysis. Evidently, the model lines describe the data from both techniques quite well. The assumption that the GISAXS spectrum is proportional to the height-height structure factor is valid if $q_z \delta h \ll 1$,[11] which is fulfilled here. It is noteworthy that the present analysis, with the inclusion of thermal noise, should be distinguished from the conventional treatment assuming the surface evolution to follow Eq. (1) instead of Eq. (3). We discuss the significance of the thermal noise in modeling the data. Both data series shown in Figs. 1 and 2 display a peak that increases in amplitude with increasing time, in keeping with the fact that the films have $G''(h) < 0$ and should roughen spontaneously. On the other hand, there are also notable deviations. By Eq. (1), the spectra should peak at a constant $q_{\parallel}=[-G''(h)/2\gamma]^{1/2}$ that maximizes $\Gamma(q_{\parallel})$ [Eq. (2)].[7] Instead, the peak position shifts continuously to smaller $q_{\parallel}$ with time. For the 80 nm film (Fig. 1), the peak position never comes to a constant; while for the 4 nm film, it does so only after $t > 480$ s (Fig. 2). We demonstrate that the continuous shift in the peak position of the surface spectra from zero time is due to thermal noise. We perform model calculations analogous to those used to produce the solid lines in Fig. 1, except that $G''(h)$ is set to zero. This setting of $G''(h)$ eliminates the component of evolution in $|\delta h(q_{\parallel},t)|^2$ due to the spinodal process. But it can also artificially reduce $\Gamma(q_{\parallel})$ substantially below the actual value if $q_{\parallel}$ is not $\geqslant q_c=[-G''(h)/\gamma]^{1/2}$ [Eq. (2)]. For $h=80$ nm, q_c ($\approx 1.7 \times 10^{-6}$ Å^{-1}), which lies outside the range of $q_{\parallel}$ studied so should not fall prey to the caveat. The calculations with $G''(h)=0$ are shown in Fig. 1 by the dashed lines, which essentially overlap with the original calculations, demonstrating the significance of thermal noise.

Figure 3 shows the data of viscosity (η) plotted versus temperature (T) measured from the $h \approx 80$ nm films by GISAXS and AFM, as well as the $h=5$ nm films by AFM. As seen, the data obtained by GISAXS and AFM give essentially the same result. The solid line, representing the pub-

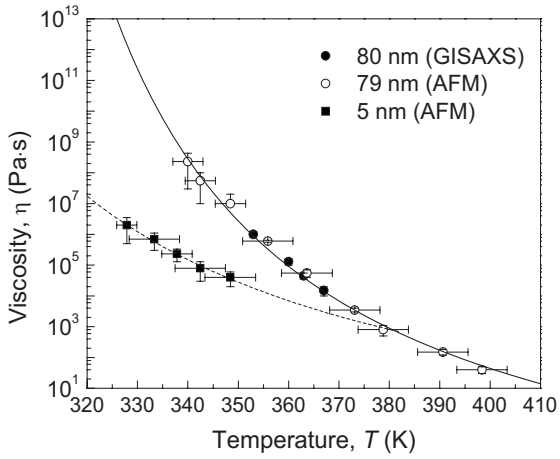

FIG. 3. Plot of η vs T of $h \approx 80$ and 5 nm films by GISAXS and AFM. Solid line represents the viscosity of the bulk. Dashed line is the best fitted line to the VFT relation.

lished data of the bulk polymer,[12] exhibits excellent consistency with the $h=80$ nm data. On the other hand, deviations with the data of the 5 nm films are notable. Specifically, the 5 nm film data fall well below the bulk value; the ratio of the latter to the former enlarges continuously from $\sim 10^2$ at 350 K to $\sim 10^7$ at 328 K. To shed some light, we fit the viscosity data to the Vogel–Fulcher–Tammann (VFT) relation commonly used to describe the dynamics near the glass transition, namely $\eta(T)=\eta(T_{\mathrm{ref}})\exp[B/(T-T_0)-B/(T_{\mathrm{ref}}-T_0)]$, where T_{ref} is an arbitrarily chosen reference temperature (=381 K here), B is a constant, and T_0 is the Vogel temperature. For PS with $M_w=2.4$ kg/mol, $\eta(T_{\mathrm{ref}})=745$ Pa s, $B=1620$ K, and $T_0=288$ K.[12] Previously, the T_g of the films was observed to decrease with decreasing h following $T_g(h)=T_g(\infty)/(1+0.82\ \mathrm{nm}/h)$.[13] For $h=5$ nm, this gives $T_g(h)=296$ K, i.e., ~40 K below the bulk T_g. We find that the data of the 5 nm films can be fitted well to the VFT relation if T_0 assumes the value of 247 K (dashed line, Fig. 3), which is also ~40 K below the bulk value. This result indicates that the observed variation in the T_g with film thickness may originate from an analogous variation in the T_0 with the film thickness.

We thank Professor K. F. Ludwig for critical reading of this paper and Dr. Y. Fujii for useful discussions. Funding supports of NSF (Grant No. DMR-0706096) and ACS Petroleum Research Fund (Grant No. 47882-AC5) are acknowledged. NSLS is supported by the U.S. Department of Energy Contract No. DE-AC02-98CH10886.

[1] C. A. Angell, Science **267**, 1924 (1995).
[2] J. L. Keddie, R. A. L. Jones, and R. A. Cory, Faraday Discuss. **98**, 219 (1994); M. Alcoutlabi and G. B. McKenna, J. Phys.: Condens. Matter **17**, R461 (2005).
[3] O. K. C. Tsui, in *Polymer Thin Films*, edited by O. K. C. Tsui and T. P. Russell (World Scientific, New Jersey, 2008), p. 267.
[4] H. Kim, A. Ruhm, L. B. Lurio, J. K. Basu, J. Lal, D. Lumma, S. G. J. Mochrie, and S. K. Sinha, Phys. Rev. Lett. **90**, 068302 (2003).
[5] Z. Jiang, H. Kim, X. Jiao, H. Lee, Y.-J. Lee, Y. Byun, S. Song, D. Eom, C. Li, M. H. Rafailovich, L. B. Lurio, and S. K. Sinha, Phys. Rev. Lett. **98**, 227801 (2007).
[6] J.-L. Masson and P. F. Green, Phys. Rev. E **65**, 031806 (2002).
[7] Y. J. Wang and O. K. C. Tsui, Langmuir **22**, 1959 (2006).
[8] H. Zhao, Y. J. Wang, and O. K. C. Tsui, Langmuir **21**, 5817 (2005).
[9] A. Vrij and J. Th. G. Overbeek, J. Am. Chem. Soc. **90**, 3074 (1968).
[10] Y. J. Wang and O. K. C. Tsui, J. Non-Cryst. Solids **352**, 4977 (2006).
[11] S. K. Sinha, E. B. Sirota, and S. Garoff, Phys. Rev. B **38**, 2297 (1988).
[12] J.-C. Majeste, J.-P. Montfort, A. Allal, and G. Marin, Rheol. Acta **37**, 486 (1998).
[13] S. Herminghaus, K. Jacobs, and R. Seemann, Eur. Phys. J. E **5**, 531 (2001).